

**DEVELOPMENT OF A MULTI-LUMEN  
DIAMETER COMMON CAROTID ARTERY  
WALL-LESS PHANTOM AND BLOOD  
MIMICKING FLUIDS FOR DOPPLER  
ULTRASOUND**

**DAKOK KYERMANG KYENSE**

**UNIVERSITI SAINS MALAYSIA**

**2021**

**DEVELOPMENT OF A MULTI-LUMEN  
DIAMETER COMMON CAROTID ARTERY  
WALL-LESS PHANTOM AND BLOOD  
MIMICKING FLUIDS FOR DOPPLER  
ULTRASOUND**

by

**DAKOK KYERMANG KYENSE**

**Thesis submitted in fulfilment of the requirements  
for the degree of  
Doctor of Philosophy**

**October 2021**

## ACKNOWLEDGEMENT

I would like to express my gratitude to The Almighty God for giving me good health, strength, wisdom, knowledge and sound mind to carry out this research work successfully. My special gratitude also goes to my main supervisor; Prof. Dr. Mohammed Zubir Mat Jafri for not only being my supervisor, but a father, mentor and a counsellor. He has provided me with guidance and support during the course of my studies and has always provided exciting discussions about research. I have learned many valuable lessons from him and will keep him as a reference for academic excellence and as a close mentor for years to come. In addition, worthy of gratitude is my co-supervisor, Dr Nursakinah Suardi who has always been there to assist me in every difficult situation and to ensure that this research exercise was fruitful. I remain eternally grateful to her for her uncountable supports and kindness, wishing her long life and prosperity in all her endeavours. I would like to acknowledge the contributions of Mr Ramlee Abd Wahab for providing the technical knowledge of my research, Mr Hazhar Hassan of medical physics laboratory for providing the necessary and convenient environment to carry out the research, all the staff of NOR laboratory, solid state and energy laboratories of school of physics, Universiti Sains Malaysia for their support in different ways. Finally, my heartfelt gratitude goes to the federal government of Nigeria, Tertiary Education Trust Fund (TETFund) and the Plateau State Government through the Plateau State University Boko for sponsoring my program. I appreciate my wife (Nanchin Kyense Dakok), children, parents and brothers for their prayers and support towards the success of my studies.

## TABLE OF CONTENTS

|  |             |
|--|-------------|
| <b>ACKNOWLEDGEMENT</b> .....                     | <b>ii</b>   |
| <b>TABLE OF CONTENTS</b> .....                   | <b>iii</b>  |
| <b>LIST OF TABLES</b> .....                      | <b>vii</b>  |
| <b>LIST OF FIGURES</b> .....                     | <b>ix</b>   |
| <b>LIST OF SYMBOLS</b> .....                     | <b>xiii</b> |
| <b>LIST OF ABBREVIATIONS</b> .....               | <b>xiv</b>  |
| <b>ABSTRAK</b> .....                             | <b>xvii</b> |
| <b>ABSTRACT</b> .....                            | <b>xix</b>  |
| <b>CHAPTER 1 INTRODUCTION</b> .....              | <b>1</b>    |
| 1.1 Background of the Study.....                 | 1           |
| 1.2 Problem Statement .....                      | 3           |
| 1.3 Objectives of Study .....                    | 5           |
| 1.4 Scope of the Research .....                  | 6           |
| 1.5 Thesis Organization .....                    | 6           |
| <b>CHAPTER 2 LITERATURE REVIEW</b> .....         | <b>7</b>    |
| 2.1 Introduction .....                           | 7           |
| 2.2 Anatomy of the Human Carotid Artery .....    | 7           |
| 2.2.1 Human Carotid Artery.....                  | 7           |
| 2.2.2 Carotid Artery Disease.....                | 10          |
| 2.2.3 Carotid Artery Phantom .....               | 12          |
| 2.2.3 (a) Walled Carotid Artery Phantoms .....   | 12          |
| 2.2.3 (b) Wall-less Carotid Artery Phantoms..... | 21          |
| 2.3 Mechanical Properties of Human tissues ..... | 29          |
| 2.3.1 Density .....                              | 29          |
| 2.3.2 Viscosity.....                             | 29          |
| 2.3.3 Elasticity.....                            | 31          |

|  |  |    |
|--|--|----|
| 2.4                                      | Acoustic Properties of Human Tissues .....   | 32 |
| 2.4.1                                    | Speed of sound .....   | 32 |
| 2.4.2                                    | Attenuation.....   | 32 |
| 2.4.3                                    | Backscattering .....   | 33 |
| 2.5                                      | Diagnostic Ultrasound.....   | 34 |
| 2.5.1                                    | Physics of Ultrasound .....  | 34 |
| 2.5.2                                    | Doppler Ultrasonography.....   | 37 |
| 2.6                                      | Doppler Ultrasound Techniques .....  | 39 |
| 2.6.1                                    | Pulse wave-mode (PW-Mode).....   | 39 |
| 2.6.2                                    | Continuous wave-mode (CW-mode) .....   | 41 |
| 2.6.3                                    | Color-mode Doppler (C-mode).....   | 41 |
| 2.6.4                                    | Power-mode Doppler .....   | 42 |
| 2.7                                      | Quantitative Doppler Technique .....   | 43 |
| 2.7.1                                    | Laminar, Turbulent and Disturbed flow .....  | 43 |
| 2.7.2                                    | Blood Flow Velocity Profiles.....  | 45 |
| 2.7.3                                    | Waveform Doppler Indices .....   | 47 |
| 2.7.4                                    | Effect of Glucose and Cholesterol on Doppler Ultrasound<br>Flow Velocity in the Carotid Artery ..... | 49 |
| 2.8                                      | Negative Effects of Ultrasound Technique .....   | 50 |
| 2.9                                      | Flow phantom Pump System .....   | 51 |
| 2.10                                     | Summary of Research Gap .....  | 53 |
| CHAPTER 3 MATERIALS AND METHODOLOGY..... |  | 55 |
| 3.1                                      | Introduction .....   | 55 |
| 3.2                                      | Chemical Items for Preparing Tissue Mimicking Material (TMM) .....                                   | 55 |
| 3.3                                      | Chemical Items for Preparing Blood Mimicking Fluid (BMF) .....                                       | 57 |
| 3.4                                      | Instruments used for Preparing and Measuring BMF and TMM.....  | 60 |
| 3.5                                      | Methodology .....  | 65 |
| 3.5.1                                    | Blood Mimicking Fluid (BMF) Preparation .....  | 66 |

|  |  |           |
|--|--|-----------|
| 3.5.1(a)                                     | Blood Mimicking Fluid with Glucose.....  | 66        |
| 3.5.1(b)                                     | Measurements of Density and Viscosity.....                                     | 68        |
| 3.5.1(c)                                     | Measurements of speed of sound, Attenuation and Backscatter power.....         | 68        |
| 3.5.1(d)                                     | Preparation of BMF with Cholesterol.....                                       | 72        |
| 3.5.2  | Fabrication of the Multi-lumen Diameter CCA wall-less Phantom .....            | 75        |
| 3.5.2(a)                                     | Construction of the Phantom Box .....  | 75        |
| 3.5.2(b)                                     | Preparation and casting of the TMM .....                                       | 77        |
| 3.5.3  | Gear Pump System.....  | 80        |
| 3.5.4  | Hitachi Ultrasound Scanning and measurements of Ultrasound Data .....          | 80        |
| 3.5.5  | Velocity error calculation.....  | 82        |
| <b>CHAPTER 4 RESULTS AND DISCUSSION.....</b> |  | <b>84</b> |
| 4.1  | Introduction .....   | 84        |
| 4.2  | Characterization of the Multi-Lumen Diameter CCA Wall-less Phantom ....        | 84        |
| 4.2.1  | Acoustic Properties of the Multi-Lumen Diameter CCA TMM Wall-less Phantom..... | 85        |
| 4.2.2  | Geometry of the TMM Wall-less Phantom Using B-mode Imaging .....               | 86        |
| 4.2.3  | Geometry of the Blood Mimicking Fluids (BMF) in the Wall-less phantom.....     | 88        |
| 4.3  | Physical and Acoustic Properties of the Blood Mimicking Fluids .....           | 91        |
| 4.3.1  | Physical and acoustic properties of BMF with Glucose .....                     | 91        |
| 4.3.2  | Physical and acoustic properties of BMF with Cholesterol.....                  | 95        |
| 4.4  | Pulse-wave and Colour Doppler measurements of Flow Velocity .....              | 99        |
| 4.4.1  | Variation between BMF Mean Velocity with Flow Rate .....                       | 100       |
| 4.4.2  | Laminar Flow and Velocity Profile Outline .....                                | 101       |
| 4.4.3  | Variation between velocity measurements and Doppler angle ....                 | 103       |

|   |  |            |
|---|--|------------|
| 4.4.4   | Measurements of PSV, EDV, PI, RI and Vm of the BMF Samples .....   | 105        |
| 4.4.4(a)  | Comparison between in-vitro and in-vivo flow indices .....   | 108        |
| 4.4.4(b)  | Effect of Change in Glucose and Cholesterol levels on Peak Systolic and End Diastolic Velocity in the Wall-less Phantoms. .... | 111        |
| 4.4.4(c)  | Applications of the PSV, EDV, PI and RI Measurements .....   | 115        |
| 4.5   | Limitations of the research study .....  | 116        |
| 4.6   | Summary .....  | 117        |
| <b>CHAPTER 5 CONCLUSION AND FUTURE RECOMMENDATIONS.....</b> |  | <b>118</b> |
| 5.1   | Conclusion.....  | 118        |
| 5.2   | Recommendations for Future Research .....  | 119        |
| <b>REFERENCES.....</b>                                      |  | <b>121</b> |
| <b>APPENDICES</b>   |  |            |
| <b>LIST OF PUBLICATIONS</b>                                 |  |            |

## LIST OF TABLES

|           | <b>Page</b>   |
|-----------|---|
| Table 2.1 | Carotid artery dimensions for healthy men an women.....9  |
| Table 2.2 | Acoustic properties of TMM and VMM .....14  |
| Table 2.3 | Percentage composition of substances used to prepare vessel mimicking material (VMM) and their uses in anthropometric atherosclerotic walled phantom ..... 18 |
| Table 2.4 | Percentage composition of substances used to prepare tissue mimicking material (TMM) and their uses in anthropometric atherosclerotic walled phantom. .... 19 |
| Table 2.5 | Percentage composition of substances used to prepare blood mimicking fluid (BMF) and their uses in anthropometric atherosclerotic walled phantom. .... 19     |
| Table 2.6 | Constituents of Konjac-Carrageenan based tissue mimicking material (TMM) for wall-les phantom.....24  |
| Table 2.7 | Acoustic properties of TMM for broadband substitution and high frequency ultrasound methods..... 24   |
| Table 2.8 | Summary of Major Research Gaps and Contributions in Filling the Gaps..... 54  |
| Table 3.1 | Chemical substances used for preparing blood mimicking fluids.....59  |
| Table 3.2 | Specifications of the BMF defined by the IEC standard (IEC, 2001) ..... 73  |
| Table 3.3 | Constituents of Konjac-Carrageenan (KC) and gelatin (from bovine skin) tissue mimicking material (TMM) for wall-les phantom..... 80                           |
| Table 4.1 | Speed of Sound of the KC and gelatine based TMM at different transducer frequencies..... 85   |



|            |   |     |
|------------|---|-----|
| Table 4.2  | Physical and acoustic properties of mixture fluid for the preparation of a blood mimicking fluid with glucose at a temperature of 37 <sup>0</sup> C.....                                  | 91  |
| Table 4.3  | Physical and acoustic properties of mixture fluid for the preparation of a blood mimicking fluid with propylene glycol and polyethylene glycol at a temperature of 37 <sup>0</sup> C..... | 97  |
| Table 4.4  | Physical and acoustic properties of mixture fluid for the preparation of a blood mimicking fluid with propylene glycol and D(+)-Glucose at a temperature of 37 <sup>0</sup> C.....        | 97  |
| Table 4.5  | Variation of Temperature with the Physical and Acoustic properties of BMF prepared with Cholesterol.....  | 99  |
| Table 4.6  | Mean velocity measurements of BMF with glucose for flow rates from 500 – 1500 ml/min across the 8 wall-less phantoms.....   | 100 |
| Table 4.7  | Mean velocity measurements of BMF with cholesterol for flowrates from 500 – 1500 ml/min across the 8 wall-less phantoms.....  | 101 |
| Table 4.8  | Variation between mean velocity of BMF samples with Doppler angle for 6.0 mm wall-less phantom.....   | 104 |
| Table 4.9  | Blood flow parameters from simulation with blood mimicking fluid with glucose.....  | 105 |
| Table 4.10 | Blood flow parameters from simulation with blood mimicking fluid with cholesterol scatterers .....  | 106 |
| Table 4.11 | Blood flow parameters from simulation with blood mimicking fluid without glucose and cholesterol.....   | 106 |
| Table 4.12 | Blood flow parameters from real human beings (Pam et al., 2015a; Pam et al.,2015b).....   | 108 |

## LIST OF FIGURES

|             | <b>Page</b>   |
|-------------|---|
| Figure 2.1  | Major arteries of the head, neck, and brain (Yvonne <i>et al.</i> , 2020)..... 8  |
| Figure 2.2  | Schematic diagram of <b>(a)</b> blood vessel structure and its components, <b>(b)</b> localized shear stress in carotid artery (Ashish <i>et al.</i> , 2019).....8                                    |
| Figure 2.3  | NASCET and ECST measurements of internal carotid artery stenosis (NASCET, 1991; Articles, 1991). ..... 11   |
| Figure 2.4  | Carotid bifurcation models with normal geometry (top) and with a 60% stenosis (bottom) by NASCET criteria (Poeppling <i>et al.</i> , 2004) ..... 14   |
| Figure 2.5  | Photograph of flow phantom. Inset shows infiltration of TMM into reticulated foam (Ramnarine <i>et al.</i> , 2001). .....222  |
| Figure 2.6  | (a) Schematic illustration and (b) photograph of empty vessel phantom mould ready for KC solution pouring (Ammar <i>et al.</i> , 2018).....27   |
| Figure 2.7  | (a) Schematic illustration and (b) photograph of vessel phantom (vessel diameter with 8 mm) with KC-based TMM and glycerol solution (Ammar <i>et al.</i> , 2018).....28                               |
| Figure 2.8  | Angle between the ultrasound beam and the direction of blood flow (Sandra , 2018) .....39   |
| Figure 2.9  | A schematic diagram showing <b>(a)</b> laminar flow and <b>(b)</b> turbulent flow (Peter <i>et al.</i> , 2019) .....43  |
| Figure 2.10 | The change in velocity profile, with distance along a rigid tube, from a blunt to a parabolic profile (Peter <i>et al.</i> , 2019).....45   |
| Figure 2.11 | Velocity patterns observed in the normal carotid bifurcation (Peter <i>et al.</i> , 2019).....46  |
| Figure 2.12 | Doppler indices derived from peak systolic velocity (S1), second systolic (S2), insicura between systole and diastole (I), peak diastole (D) and end-diastole (d) velocities (Maulik, 2005). ..... 49 |
| Figure 2.13 | Gear pumps, (a) GA-V21 pump system, (b) GJ-N25 pump system (Zhou <i>et al.</i> , 2017). .....52   |

|             |   |    |
|-------------|---|----|
| Figure 3.1  | Ultrasonic Echoscope (GAMPT-Scan) systems (b) Analytical electronic balance, (c) Density Meter (DMA35) .....  | 62 |
| Figure 3.2  | (a) Electronic Rotational Viscometer, (b) Magnetic stirrers, (c) Pressing Rotary Hand Beater Whisk stainless Steel Mixer .....  | 63 |
| Figure 3.3  | Gear pump multi-flow (GAMPT) system.....  | 64 |
| Figure 3.4  | A digital Hitachi Ultrasound Machine (HI Vission).....  | 65 |
| Figure 3.5  | Magnetic stirring mixing the components properly and to become homogeneous .....  | 67 |
| Figure 3.6  | (a) Density meter (DMA 35) to measure the density of the aqueous solutions, (b) Rotational Viscosity Meter measuring the viscosity of the mixture fluids, (c) Measurement of the acoustic properties of solutions using the A-scan Gampt technique..... | 70 |
| Figure 3.7  | Flowchart Summarizing the Procedure for Preparing a BMF with Glucose.....   | 71 |
| Figure 3.8  | Flowchart Summarizing the Procedure for Preparing a BMF with Cholesterol.....   | 74 |
| Figure 3.9  | Procedures for preparing a vascular wall-less phantom; (a) Phantom box with horizontal rods, (b) cooking of TMM, (c) casting of the TMM inside the phantom box .....  | 76 |
| Figure 3.10 | Flowchart Summarizing the Procedure for Preparation and Casting of Tissue Mimicking Material.....   | 79 |
| Figure 3.11 | Ultrasound measurements of hemodynamic parameters (PSV, EDV, Vm, PI and RI) using the Hitachi ultrasound machine .....  | 82 |
| Figure 4.1  | Figure 4.1: Linear graph of the attenuation at different frequencies.....   | 86 |
| Figure 4.2  | B-Mode (a) transverse image of lumen diameter without the BMF, (b) longitudinal image of lumen diameter without the BMF.....  | 87 |
| Figure 4.3  | Figure 4.3: A Bar-chart showing pixel intensity distribution of the TMM at different frequencies .....  | 88 |

|             |  |     |
|-------------|--|-----|
| Figure 4.4  | Gray-scale images of longitudinal sections of (a) BMF with glucose, (b) BMF with cholesterol during flow measurements.....                                     | 89  |
| Figure 4.5  | Colour-mode appearance of the BMF inside the phantom .....   | 90  |
| Figure 4.6  | Motion-mode (M-mode) image of both BMF and TMM during flow measurement.....  | 90  |
| Figure 4.7  | Linear graphical representation of relationship between Density and D(+)-Glucose Concentration (DGCon).....  | 93  |
| Figure 4.8  | Relative backscatter from BMF under uniform flow plotted against particle concentration for Poly (4-methylstyrene) particles of size 3-8 $\mu\text{m}$ . ..... | 94  |
| Figure 4.9  | Appearance of Poly (4-methylstyrene) scatter particles inside the BMF fluid.....   | 95  |
| Figure 4.10 | Relative backscatter from BMF under uniform flow plotted against particle concentration for Poly Cholesterol particles of size $\leq 20\mu\text{m}$ .....      | 98  |
| Figure 4.11 | Velocity profile of BMF with glucose in the 8.0 mm wall-less phantom.....  | 102 |
| Figure 4.12 | Velocity profile of BMF with cholesterol in the 8.0 mm wall-less phantom .....   | 103 |
| Figure 4.13 | Peak systolic velocity values for the blood samples; PSV1 (BMF with glucose), PSV2 (BMF with cholesterol), PSV3 (human blood) in the 8 lumen diameters.....    | 109 |
| Figure 4.14 | End diastolic velocity values for the blood samples; EDV1 (BMF with glucose), EDV2 (BMF with cholesterol), EDV3 (human blood) in the 8 lumen diameters.....    | 109 |
| Figure 4.15 | Average (mean) velocity values for the blood samples; Vm1 (BMF with glucose), Vm2 (BMF with cholesterol), Vm3 (human blood) in the 8 lumen diameters.....      | 110 |
| Figure 4.16 | Variations between Peak Systolic Velocity and glucose level across the lumen diameters from 4.5 mm to 8.0 mm.....  | 112 |

|             |   |     |
|-------------|---|-----|
| Figure 4.17 | Variations between Peak Systolic Velocity and cholesterol level across the lumen diameters from 4.5 mm to 8.0 mm..... | 113 |
| Figure 4.18 | Variations between End Diastolic Velocity and Glucose level across the lumen diameters from 4.5 mm to 8.0 mm.....     | 113 |
| Figure 4.19 | Variations between End Diastolic Velocity and Cholesterol level across the lumen diameters from 4.5 mm to 8.0 mm..... | 114 |

## LIST OF SYMBOLS

|                   |                                 |
|-------------------|---------------------------------|
| c                 | Speed of sound                  |
| cm/s              | Centimetre per second           |
| dB/cm             | decibel per centimetre          |
| f                 | frequency                       |
| g/cm <sup>3</sup> | Gram per centimetre cube        |
| Kg/m <sup>3</sup> | Kilogram per meter cube         |
| KHz               | Kilo-Hertz                      |
| KPa               | Kilo-Pascal                     |
| mg/dl             | Millilitre per decilitre        |
| ml/min            | Millilitre per minute           |
| mPa.s             | Mill-pascal second              |
| MHz               | Mega-Hertz                      |
| ml/s              | Millilitre per second           |
| mm                | Millimetre                      |
| Ns/m <sup>2</sup> | Newton second per meter square  |
| m/s               | Meter per second                |
| Re                | Reynold's number                |
| T                 | period                          |
| v                 | Velocity of flow                |
| $\alpha$          | Alpha (attenuation coefficient) |
| $\lambda$         | Lamda (wavelength)              |
| $\mu\text{m}$     | Micro-meter                     |
| $\theta$          | Theta (angle)                   |

## LIST OF ABBREVIATIONS

|                                |   |
|--------------------------------|---|
| ABS                            | Acrylonitrile butadiene styrene                           |
| Al <sub>2</sub> O <sub>3</sub> | Aluminium oxide   |
| A-mode                         | Amplitude-modulation                                      |
| A-scan                         | Amplitude-scan  |
| AVI                            | Augmented velocity index                                  |
| BKC                            | Benzalkonium chloride                                     |
| B-mode                         | Brightness-modulation                                     |
| BMF                            | Blood-mimicking fluid                                     |
| CAM                            | Computer aided manufacturing                              |
| CCA                            | Common carotid artery                                     |
| CHO                            | Total cholesterol   |
| C-mode                         | Color-modulation  |
| CW-mode                        | Continuous wave-modulation                                |
| DG                             | D(+)-Glucose  |
| DU                             | Doppler ultrasound  |
| ECA                            | External carotid artery                                   |
| EDV                            | End diastolic velocity                                    |
| ECST                           | European carotid surgery trial                            |
| FFT                            | Fast Fourier Transform                                    |
| GAMPT                          | German Society for Applied Medical Physics and technology |
| HDI                            | High Definition Imaging                                   |
| HDL                            | High density lipoproteins                                 |
| ICA                            | Internal carotid artery                                   |
| IEC                            | International electrochemical commission                  |

|                |   |
|----------------|---|
| IMT            | Intima-media thickness                                  |
| KC             | Konjac-carrageenan                                      |
| LDL            | Low density lipoproteins                                |
| M-mode         | Motion-modulation                                       |
| NASCET         | North American Symptomatic Carotid Endarterectomy Trial |
| PE             | Pulse echo  |
| PEG            | Polyethylene glycol                                     |
| PG             | Propylene glycol  |
| PI             | Pulsatility index                                       |
| PSV            | Peak systolic velocity                                  |
| PRF            | Pulsed repetition frequency                             |
| PRI            | Pulsed repetition index                                 |
| PVA            | Polyvinyl alcohol                                       |
| PVA-C          | Polyvinyl alcohol cryogel                               |
| PVC            | Polyvinyl chloride                                      |
| PW-mode        | Pulsed wave-modulation                                  |
| RI             | Resistivity index                                       |
| SiC            | Silicon carbide   |
| TAMV           | Time average mean velocity                              |
| TIA            | Transient ischemic attack                               |
| ToF            | Time of flight  |
| TMM            | Tissue-mimicking material                               |
| TRIG           | Triglycerides   |
| VEI            | Velocity elastic index                                  |
| V <sub>m</sub> | Mean velocity   |



|     |                           |
|-----|---------------------------|
| VMM | Vessel-mimicking material |
| VRI | Velocity reflection index |
| w/w | Weight per Weight         |

**PEMBANGUNAN FANTOM ARTERI KAROTID LAZIM TANPA DINDING  
MULTI DIAMETER LUMEN DAN BENDALIR TIRUAN DARAH UNTUK  
ULTRABUNYI DOPPLER**

**ABSTRAK**

Aliran fantom dengan geometri anatomi realistik dan keserasian akustik yang tinggi dengan saluran darah sebenar merupakan alat yang boleh dipercayai dalam kajian ultrabunyi vaskular. Suatu fantom baharu bagi karotid arteri biasa (CCA) tanpa dinding dengan diameter multi-lumen dibina, yang digunakan untuk kajian halaju aliran ultrabunyi menggunakan cecair darah tiruan (BMF) dengan kandungan glukosa dan kolesterol. Fantom dibina dengan 8 diameter lumen dari 4.5 mm hingga 8.0 mm berkedalaman imbasan 7.5 mm, semuanya dalam geometri karotid manusia biasa. Bahan tisu tiruan (TMM) terdiri daripada *konjac*, *carrageenan* dan gelatin sebagai komponen asas yang dicampur dengan komponen lain yang sesuai. BMF telah disediakan dengan mencampurkan propylene glycol (PG), D(+)-glukosa (DG) dan poly (4-methylstyrene) berselerak dalam air suling untuk BMF pertama, diikuti dengan menggantikan poli (4-methylstyrene) dengan kolesterol untuk membentuk BMF pertama, diikuti dengan menggantikan poli (4-methylstyrene) dengan kolesterol untuk membentuk BMF kedua. Fantom yang dibina telah diimbas menggunakan mesin ultrabunyi untuk mengukur kelajuan aliran dan petunjuk lain melalui lumens dan juga untuk menguji kualiti phantom. Fantom didapati mantap, anjal dan kuat dengan kelajuan bunyi dan attenuasi masing-masing pada  $1548.20 \pm 0.02$  m/s dan  $0.35 \pm 0.02$  dB/cm.MHz masing-masing pada kekerapan 5 MHz. BMF yang terbaik dengan glukosa dihasilkan mempunyai ketumpatan  $1.04 \pm 0.01$  g/cm<sup>3</sup>, kelikatan  $4.30 \pm 0.05$  mpa.s, kelajuan bunyi  $1580.00 \pm 0.30$  m/s dan

attenuasi  $0.02 \pm 0.01$  dB/cm pada 5MHz. BMF kedua dengan kolesterol sebagai zarah berselerak mempunyai ketumpatan  $1.07 \pm 0.01$  g/cm<sup>3</sup>, kelikatan  $4.50 \pm 0.04$  mPa.s, kelajuan bunyi  $1600.00 \pm 0.50$  m/s dan attenuasi  $0.02 \pm 0.01$  dB/cm. Ukuran aliran kelajuan dan indeks BMF melalui *phantom* CCA yang sihat dari saluran darah sebenar. PSV bagi kedua-dua sampel BMF adalah dari 40.00 cm/s hingga 134.00 cm/s, manakala EDV adalah dari 10.00 cm/s hingga 39.00 cm/s untuk 8.00 mm hingga 4.50 mm diameter fantom. Nilai PI dan RI juga berada dalam piawaian yang boleh diterima di peringkat antarabangsa untuk arteri yang sihat. Hubungan pembalikkan ditemui antara diameter lumen dengan PSV, EDV dan Vm.

**DEVELOPMENT OF A MULTI-LUMEN DIAMETER COMMON CAROTID  
ARTERY WALL-LESS PHANTOM AND BLOOD MIMICKING FLUIDS  
FOR DOPPLER ULTRASOUND**

**ABSTRACT**

Flow phantoms with anatomically realistic geometry and high acoustic compatibility with real vessels are reliable tools in vascular ultrasound studies. A new common carotid artery (CCA) wall-less phantom with multi-lumen diameters has been presented to be used for ultrasound flow velocity studies using blood mimicking fluids (BMF) containing glucose and cholesterol. The phantom was constructed with 8 lumen diameters from 4.50 mm to 8.00 mm with a scanning depth of 7.5 mm, all within normal human carotid geometry. The tissue mimicking material (TMM) consists of konjac, carrageenan and gelatine as basic components mixed with other suitable components such as distilled water, aluminium oxide, potassium chloride, silicon carbide, glycerol and benzalkonium chloride. The BMF was prepared by mixing propylene glycol (PG), D(+)-glucose (DG) and poly (4-methylstyrene) scatters in distilled water for the first BMF, followed by replacing the poly (4-methylstyrene) with cholesterol to form the second BMF. The constructed phantom was scanned using ultrasound machine to measure flow velocities, pulsatility index (PI) and resistivity index (RI) through the lumens and to test the effectiveness of the phantom. The phantom was found to have a speed of sound and attenuation of  $1548.20 \pm 0.02$  m/s and  $0.35 \pm 0.02$  dB/cm respectively at a frequency of 5 MHz. A very good BMF with glucose was produced having a density of  $1.04 \pm 0.01$  g/cm<sup>3</sup>, viscosity of  $4.30 \pm 0.05$  mpa.s, speed of sound of  $1580.00 \pm 0.30$  m/s and attenuation of  $0.02 \pm 0.01$  dB/cm at 5MHz. The second BMF with cholesterol as scatter particles has a density of  $1.07 \pm 0.01$  g/cm<sup>3</sup>, viscosity of

4.50±0.04 mPa.s, speed of sound 1600.00±0.50 m/s and attenuation of 0.02±0.01 dB/cm. Measurements of BMF flow velocities PI and RI through the phantom resemble those of healthy CCA of real vessels. Peak systolic velocity (PSV) for both BMF samples were from 40.00 cm/s to 134.00 cm/s, while end diastolic velocity (EDV) were from 10.00 cm/s to 39.00 cm/s for 8.00 mm to 4.50 mm diameter phantoms. PI and RI values were also within internationally acceptable standards for healthy arteries. An inverse relationship was found between the lumen diameter with the PSV, EDV and mean velocity ( $V_m$ ), while there was no much change in the BMF flow in the carotid artery at different levels of glucose/cholesterol. In conclusion, a multi-lumen diameter CCA wall-less phantom as well as BMF with glucose and cholesterol were produced with useful applications in Doppler ultrasound (DU) imaging.

# CHAPTER 1

## INTRODUCTION

### 1.1 Background of the Study

The human carotid arteries are elastic vessels found on the left and right neck each coming from the brachio-cephalic trunk into common carotid arteries (CCA), then branches into the internal and external carotid arteries. The internal carotid arteries (ICA) provides the organs located inside the cranium with oxygenated blood, while the external carotid arteries (ECA) ensure that the face is adequately provided with blood (Secchi, 2010; Lee, 2013). The vertebral artery is also found within the neck and it ensures that the brain is supplied with blood when the ICA is deficient or deformed by diseases (Holen, 1985; Boekhoven, 2015). A healthy CCA has an average diameter of 6 mm with a wall thickness of about 1 mm (Denarié *et al.*, 2000; Limbu *et al.*, 2006; Dizaji *et al.*, 2009).

A phantom is an artificial object used to mimic whole or parts of the human body. New ultrasound systems are tested to know their effectiveness using ultrasound phantoms, beside using them in training sonographers and in researches on new methods of studying diseases related to the carotid artery (Culjat *et al.*, 2010; Pereira *et al.*, 2020; Ammar *et al.*, 2020a). For a carotid artery phantom to be properly designed and constructed, the physical and acoustic properties of real human vessels and tissues must be taken into consideration (Culjat *et al.*, 2010; Oglat *et al.*, 2017; Malone *et al.*, 2020; Sabri *et al.*, 2020). This means that the tissue mimicking material (TMM), vessel mimicking material (VMM) and the blood mimicking fluid (BMF) that make up a carotid artery phantom must have values of speed of sound, viscosity, density, attenuation ( $\alpha$ ) and backscatter close to the internationally accepted standards by the International Electrochemical Commission,

61685 (IEC, 2001). Any phantom with physical and acoustic properties far from this international standard makes the Doppler systems not being able to image stationary objects, moving objects and fluids respectively ( Browne *et al.*, 2003; Ramnarine *et al.*, 2004; Culjat *et al.*, 2010; ).

Measurements of peak systolic velocity (PSV), end diastolic velocity (EDV), and PSV/EDV ratio are significant since blood flow velocity is the primary Doppler parameter considered majorly for categorizing degree of stenosis in arteries (Mehra, 2010). A normal PSV range in CCA is from 60–125 cm/s, above or below this range there may be some stenosis present in the CCA or some obstruction must have occurred (Roman *et al.*, 2006; Chavhan *et al.*, 2008; Roddy, 2010; Oglat *et al.*, 2018c). Normal EDV range in CCA is between 15 and 35 cm/s, the resistivity index (RI) between 0.72 and 0.84, and pulsatility index (PI) between 0.98–1.94 (Mikkonen *et al.*, 1997; Chavhan *et al.*, 2008; Oglat *et al.*, 2018b; Oglat *et al.*, 2018c; Ammar *et al.*, 2018c). Any value above or below these ranges of values may indicates a diseased artery or error associated with the measuring instrument/procedure.

Real blood is composed of about 55% plasma and 45% formed elements. The formed elements consist of red blood cells, white blood cells, platelets and other insoluble substances such as cholesterol; while the plasma is made up of about 90% serum and 10% other soluble substances involving proteins and glucose (Lee & Fine, 2007; Petersson, 2018). Because cholesterol is an insoluble particle in the blood, its movement within blood vessels like arteries makes it a risk factor of cardiovascular disease known as atherosclerosis or hardening of the artery wall by cholesterol deposits (stenosis) (Vasudevan *et al.*, 2013). These deposits (plaques) block the smooth flow of blood into the brain and face with time, with an end result of stroke (Alvim *et al.*, 2017; Alessandro *et al.*, 2019). The presence of glucose or sugar in the

blood stream provides the energy needed by the body to function, while cholesterol is important in body building. Excess of glucose in the blood can lead to diabetes classified as type 1 or type 2 depending on its effects on the human health. In the United states and Asia, type 2 diabetes has been a major cause of deaths (Dall *et al.*, 2003; Sarah *et al.*, 2004), therefore it is considered as one of the major cardiovascular risk factors resulting to transient ischemic stroke (Rita *et al.*, 2015; Flora & Nayak, 2019; Hamid *et al.*, 2019; Bochra *et al.*, 2020).

## **1.2 Problem Statement**

Doppler ultrasound has been extensively used in medical applications involving evaluation of carotid artery stenosis assessed by measurements of blood flow velocity, resistances and wall shear stress (Cheng *et al.*, 1993; Holen, 1985; Oglat *et al.*, 2018b). The degree of stenosis is measured by the narrowing of the lumen in the ICA caused by plaques and other solid deposits on the wall of the arteries. The gray-scale and Doppler ultrasound (DU ) examination of the arteries categorizes the degree of stenosis to be normal (no stenosis, *ICA PSV* < 125 *cm/s* and no visible plaque), 50% stenosis (*ICA PSV* < 125 *cm/s* and plaque is visible), 50%-60% stenosis (*ICA PSV* of 125 – 230 *cm/s* with visible plaque and narrowing of lumen), 70% stenosis to near occlusion (*ICA PSV* > 230 *cm/s* with visible plaque and narrowing of lumen), near occlusion and finally total occlusion (Grant *et al.*, 2003; Shivani Garg *et al.*, 2016; Samrin *et al.*, 2017).

However, a major shortcoming or gap in this study is lack of reliable Doppler ultrasound criteria for grading the severity of stenosis using information on blood flow velocities in the CCA ( Slovut *et al.*, 2010; Denis *et al.*, 2013; Ronny *et al.*, 2019). In vitro researches using carotid artery phantoms for studying the degree of



stenosis have also put their concentration on the use of PSV in the ICA as one of their primary considerations for plaque assessment (Lai *et al.*, 2013; Galluzzo *et al.*, 2015; Adrian *et al.*, 2016; Onaizah *et al.*, 2017; Filippou and Tsoumpas, 2018; Chee *et al.*, 2018; Chayer *et al.*, 2019; Elvira *et al.*, 2019). Therefore, there is need to conduct a research on the blood flow velocity with a view to using it to examine the level of severity of stenosis in the CCA. To do this, a multi-lumen diameter CCA phantom is needed with diameters ranging between 4.0 mm and 8.0 mm (normal range for a healthy CCA lumen diameter). A relationship between flow velocities in the CCA phantom and lumen diameter can be instrumental in achieving this objective.

Atherosclerosis is characterized by changes in the composition of the arterial walls that lead to the build-up of plaque, which consists of lipids, cholesterol, calcium, and other substances (such as glucose) found in the blood (Peter *et al.*, 2011; Ahmed *et al.*, 2013). Human blood has cholesterol and glucose as part of the components of its plasma and serum. High levels of these two components result to medical conditions known as hypercholesterolemia and hyperglycemia respectively (Kenneth *et al.*, 1990; Rita *et al.*, 2015), but there is no scientific report on the effects of high levels of glucose and cholesterol on flow velocity in the carotid artery. A BMF is required to simulate the real blood which will be pumped through the CCA phantom. Existing BMF are made of substances such as orgasol particles, nylon particles, sephadex or Polystyrene particles mixed in the right proportions with distilled water, glycerol dextran and surfactant. A limitation associated with previous BMF samples is the non-inclusion of cholesterol and glucose as part of the chemical items needed in the preparation; hence, the need to have a new BMF with these substances for DU analysis of blood flow velocities and resistances in the CCA is

important. No in-vitro research has ever reported a comparison between flow velocity of BMF in the CCA phantom in relation to different lumen sizes with blood flow in real human CCA with different lumen diameters. Therefore, an in-vitro and in-vivo comparison of real blood flow and BMF flow velocity in relation to various diameters is important.

The significance of this study is found in the fabrication and performance testing of series of diagnostic ultrasound phantoms which are potentially used in clinical setting especially for quality testing purposes and for training of operators in the field of ultrasound. The samples prepared can be potentially used as phantom for diagnostic ultrasonography purposes and for research training.

### **1.3 Objectives of Study**

This research is aimed at fabricating a TMM CCA wall-less phantom with different lumen diameters to study BMF flow velocity and resistances using DU technique to be applied in the assessment of stenosis in the CCA. The relevant objectives of this research are:

- (i) To design, construct and characterised a multi-lumen diameter TMM wall-less phantom and BMF samples that mimics the real human vessels
- (ii) To compare measured flow velocities and resistances of BMF samples with those of real vessel flows
- (iii) To correlate the flow velocities of the BMF samples with the CCA lumen diameter

#### **1.4 Scope of the Research**

This research is centred on fabricating a TMM wall-less phantom to mimic the CCA of humans. This phantom does not involve a VMM. BMF samples prepared are made up of different concentrations of glucose and cholesterol. Only DU measurements such as PSV, EDV, mean velocity ( $V_m$ ), PI and RI have been considered. Measurements such as shear stress, shear rate and elastic modulus of the phantom are not included in this study. Correlation analysis was carried out between BMF flow velocities and lumen diameter, while a comparison between flow velocities of the BMF samples with flow velocities of real vessels was done to characterised the phantoms.

#### **1.5 Thesis Organization**

The thesis is outlined into five chapters. Chapter 1 gives the background of the study, statement of the research problem, research aim and objectives, scope of the study and thesis organization. It explains the backbone and direction of the study. Chapter 2 provides a concise and comprehensive literature review with theoretical background on key areas related to the topic of the research. These areas include anatomy of the human carotid artery, mechanical and acoustic properties of human tissues, carotid artery phantoms (walled and wall-less) with their TMM and BMF materials, DU techniques for measurements of hemodynamic parameters. Chapter 3 presents a detailed list of apparatus needed for the research study and a concrete methodology on arrangement, protocol and acquisition of data. Chapter 4 is a presentation of results obtained and discussion of the analysed results in relation to established standards. Finally, chapter 5 is a conclusion and recommendations for further research.

## **CHAPTER 2 LITERATURE REVIEW**

### **2.1 Introduction**

Researches on DU applications have gained more attention recently, especially on in-vitro studies using phantoms of different biological organs and tissues. A good knowledge of the basic concepts related to ultrasound techniques and their applications is needed to enhance a result-oriented research. This chapter presents a detailed review on concepts such as the human carotid artery anatomy, mechanical and acoustic properties of human tissues and basic knowledge on diagnostic ultrasound.

### **2.2 Anatomy of the Human Carotid Artery**

In-vivo and in-vitro studies deal with researches involving life animals and phantoms that simulate the basic functions of some parts or whole system of animals. We will consider the anatomy of real human carotid artery and phantoms that mimic the carotid arteries.

#### **2.2.1 Human Carotid Artery**

The human carotid artery is an elastic vessel found on both sides of the neck originating from the brachio-cephalic trunk. Each CCA divides to form the ECA and ICA (with a bifurcation angle of  $50^{\circ}$ ), supplying the face and brain with oxygenated blood and nutrients as shown in figure 2.1. The ICA usually has no branching vessels in the neck and supplies oxygen rich blood to the brain, while the ECA, which supplies the facial musculature, has multiple branches in the neck. The carotid bifurcations as well as internal carotid arteries are more liable to development of atherosclerotic plaques. The left and the right CCA varies among individuals

particularly at the point where the CCA on the left neck originating from the aortic arch and at the fourth or fifth cervical vertebra where the carotid artery divides (Secchi, 2010; Albers *et al.*, 2019). Like other arteries, the carotid artery is made up of three (3) layers namely: tunica intima, media and the adventitia (Figure 2.2a), while its relative tissue makeup is about 8% endothelium, 32% elastic tissues, 44% smooth muscle cells and 16% fibrous tissues (Elaine & Katja, 2013; McNally and McLaughlin, 2020).

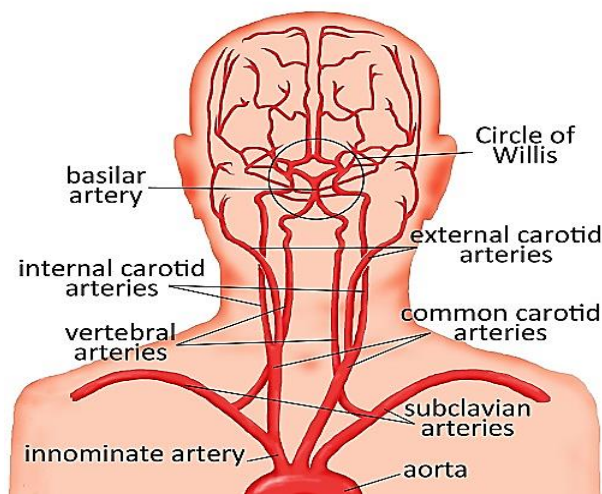


Figure 2.1: Major arteries of the head, neck, and brain (Yvonne *et al.*, 2020)

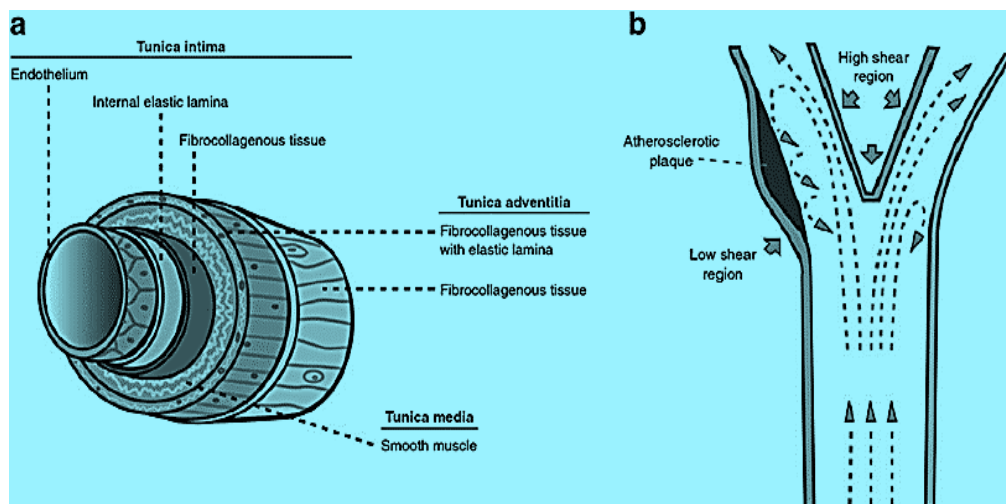


Figure 2.2: Schematic diagram of (a) blood vessel structure and its components, (b) localized shear stress in carotid artery (Ashish *et al.*, 2019).

Table 2.1 summarizes the dimensions of the carotid artery for both men and women.

Table 2.1: Carotid artery dimensions for healthy men and women (Krejza *et al.*, 2006a; Krejza *et al.*, 2006b; Limbu *et al.*, 2006; Tuncer, 2018; Choudhry *et al.*, 2016)

| <b>Carotid Artery Dimension</b>  | <b>Men</b> | <b>Women</b> |
|--|------------|--------------|
| Left CCA diameter (mm)   | 6.52±0.98  | 6.10±0.80    |
| Right CCA diameter (mm)  | 6.30±0.80  | 6.10±0.70    |
| Left ICA diameter (mm)   | 5.11±0.87  | 4.66±0.78    |
| Right ICA diameter (mm)  | 6.00±0.9   | 5.80±0.79    |
| Left ECA diameter (mm)   | 4.90±0.10  | 4.70±0.2     |
| Right ECA diameter (mm)  | 5.10±0.80  | 4.90±0.90    |
| Length of left carotid artery from aortic arch to the skull base (cm)  | 18.00±2.10 | 17.30±1.20   |
| Length of right carotid artery from aortic arch to the skull base (cm) | 22.20±1.50 | 20.80±1.80   |
| Length of left CCA from aortic arch to the skull base (cm)             | 12.40±1.20 | 11.10±0.60   |
| Length of right CCA from aortic arch to the skull base (cm)            | 13.60±0.85 | 12.00±0.70   |

The intima media thickness (IMT) of the carotid artery for a healthy human has a value from 0.5 mm to 0.7 mm while a value greater than or equal to 1.0 mm is associated with increased risk of cardiovascular complications (Ravi *et al.*, 2014; Mugada & Kolakota, 2019). Measurements of carotid artery diameter, IMT and length are good parameters for assessing carotid abnormality, hence a necessary aspect for researches and studies (Sedaghat *et al.*, 2018).

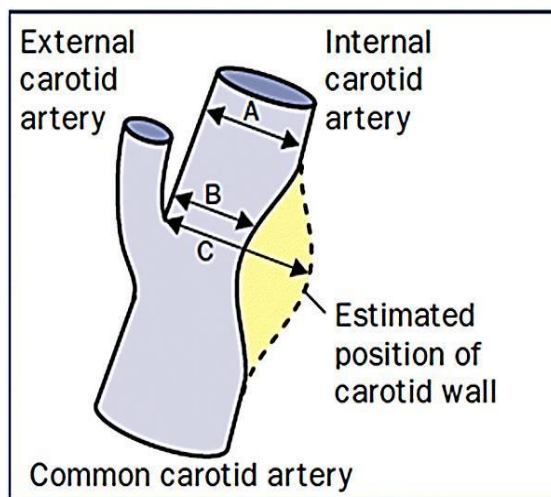
### 2.2.2 Carotid Artery Disease

Carotid artery disease occurs when fatty deposits (plaques) clog the blood vessel (carotid artery) that delivers blood to the brain and head, this disease is referred to as Atherosclerosis or stenosis. Atherosclerosis is a systemic disease characterized by thickening of the arterial wall with accumulation of cholesterol in the intima, which later leads to calcifications. The blockage increases the risk of stroke, a medical emergency that occurs when blood supply to the brain is interrupted or seriously reduced (Safar and Frohlich, 2007; Toth & Cannon, 2019). Stroke is one of the leading causes of morbidity and mortality in China and many other countries in Asia (Yilu *et al.*, 2018), and it normally comes without any early warning signs. Of the two types of strokes (ischemic and hemorrhagic), only ischemic stroke is correlated with carotid atherosclerosis mostly caused by either of the two mechanisms, thrombosis or embolization leading to complete occlusion of the carotid artery. Notable among the risk factors of carotid atherosclerosis are; bad lipids (high low density lipoproteins, triglycerides and low high density lipoproteins), hypertension, smoking, obesity (high body mass index values), diabetes physical inactivity, age and recently, snoring ( Deeb *et al.*, 2018; Matthijs *et al.*, 2020).

These risk factors lead to high value of carotid IMT of greater than 1mm as a result of formation of calcified plagues within the intima and media of the carotid wall (Pastori *et al.*, 2019). The plaques keep accumulating and at a certain moment, the growth cannot be compensated anymore resulting in the narrowing of the carotid lumen (figure 2.2b). A new set of vulnerable plaques then develops containing lipids and calcifications with a thin fibrous cap. When mechanical forces in the cap due to blood pressure and blood flow exceed the maximal strength of the cap, it will rupture leading to thrombus formation into the intracranial circulation. This rupture of the

atherosclerotic plague of the carotid artery can result in neurological events like the transient ischemic attack (TIA) or ischemic stroke (Ashish *et al.*, 2019). This research studies the effect of the narrowing of the CCA on blood flow velocity with the aid of phantoms contrary to most researchers that centred their research of stenosis on the carotid bulb and the ICA only (Hase *et al.*, 2019; Hyuk *et al.*, 2019; Dominika *et al.*, 2019).

Percentage stenosis can also be assessed base on the level of narrowing of the lumen of the ICA and the bifurcation bulb as stipulated by North American Symptomatic Carotid Endarterectomy Trial (NASCET) (NASCET, 1991) and European Carotid Surgery Trial (ECST) (Articles, 1991) shown in figure 2.3. Comparing the results obtained by NASCET and ECST, a great difference is observed but both methods have found useful applications in carotid endarterectomy.



(a)

| NASCET  | ECST |
|---|------|
| 30  | 65   |
| 40  | 70   |
| 50  | 75   |
| 60  | 80   |
| 70  | 85   |
| 80  | 91   |
| 90  | 97   |
| Approximate equivalent degrees of internal carotid artery stenosis used in NASCET and ECST according to recent direct comparisons |      |

(b)

$$NASCET \% Stenosis = \frac{A-B}{A}, ECST \% Stenosis = \frac{C-B}{C}$$

Figure 2.3: NASCET and ECST measurements of internal carotid artery stenosis (NASCET, 1991; Articles, 1991).



### 2.2.3 Carotid Artery Phantom

Carotid artery phantoms can be fabricated either as wall-phantoms or wall-less phantoms.

#### 2.2.3 (a) Walled Carotid Artery Phantoms

Walled phantoms for DU studies are made up of TMM, BMF and VMM with acoustic properties close to soft tissues, blood and vessel wall respectively (Hoskins, 2008; Geoghegan *et al.*, 2012; Sabri *et al.*, 2020). This means that for a walled phantom, the BMF flows through the VMM. Flow phantoms developed before the year 2000 were made up of straight tubes designed using shrinking tubes, tapers or rods (Patterson and Foster, 1983; Cali and Robberts, 1985; McDicken, 1986; Rickey *et al.*, 1995; Guo and Fenser, 1996; Hoskins, 1997).

An example of a flow test simulator was constructed to represent a non-stenosed CCA which used a tube of internal diameter 7.9 mm with wall thickness 0.1 mm placed inside a 15 mm TMM medium depth (Steinman *et al.*, 2001). This phantom was designed to study maximum velocity errors linked with measurements using DU systems. The BMF used has a density and viscosity of 1.02 g/cm<sup>3</sup> and 3.6 mPa.s at room temperature respectively (Rickey *et al.*, 1995) mixed with nylon scatterers of 5 mm diameter (Ramnarine *et al.*, 1998). This BMF was passed through the test phantom with a steady flow of 7.31 ml/s (Shehada *et al.*, 1993). The maximum velocity estimation error was calculated using equation 2.1 (Steinman *et al.*, 2001):

$$v_{est-max} = \frac{v_{d-max} - v_{t-max}}{v_{t-max}} \times 100\% \quad (2.1)$$

Where  $v_{d-max}$  is the highest velocity, while  $v_{t-max}$  is the real peak velocity. A positive and negative value for  $v_{est-max}$  represents an overestimation error and an

underestimation error respectively. Results from this research (Steinman *et al.*, 2001) suggest that the effects of Doppler angle and intrinsic spectral broadening are the major sources of DU errors and should be the focus of future efforts to improve the accuracy of flow measurements. It was found out that the effect of transducer focal depth, intra-transducer, intra-machine, inter-machine and beam-steering did not significantly contribute to maximum velocity estimation errors. Apart from Doppler angle and spectral broadening as major sources of velocity estimation errors, it is suggested that human inexperience in carrying out US measurements could be a major source of error estimation (Steinman *et al.*, 2001).

Poepping *et al.*, 2004 constructed a phantom with silicone as the VMM while cellulose particles were added as Scatterers to test for the acoustic properties with ultrasound B-mode technique. The TMM was a combination of aluminium oxide ( $\text{Al}_2\text{O}_3$ ) and silicon carbide (SiC) to achieve the attenuation and backscatter properties (Teirlinck *et al.*, 1998; Ramnarine *et al.*, 2001), a high-gel strength agar (Rickey *et al.*, 1995) and formaldehyde as a preservative (Blechinger *et al.*, 1988; Smith *et al.*, 1999). The BMF used in this work was the one described by Ramnarine *et al.*, 1998. The vessel geometries used in fabricating this phantom were to simulate a carotid artery with bifurcation established by Smith *et al.*, 1996. It consisted of a lost-material casting technique to create two moulds with the required carotid dimension ( Smith *et al.*, 1999; Poepping *et al.*, 2002). The plaques were introduced by injecting more elastic polymer around the bulb of the ICA where soft and hard plaques were achieved by changing the quantity of scatter materials in relation to the TMM and VMM. These procedures produced healthy or normal phantom and a stenosis phantom with 60% stenosis at the ICA bulb (Figure 2.4). Both the TMM and VMM had acoustic properties as shown in table 2.2.

Table 2.2: Acoustic properties of TMM and VMM (Steinman *et al.*, 2001)

| Acoustic Properties                 | TMM                | VMM                 |
|-------------------------------------|--------------------|---------------------|
| Attenuation ( $\text{dBcm}^{-1}$ )  | $0.56 \pm 0.20$    | $3.50 \pm 0.10$     |
| Speed of Sound ( $\text{ms}^{-1}$ ) | $1539.00 \pm 4.00$ | $1020.00 \pm 20.00$ |

The phantoms showed excellent physical stability over time with no gross changes observed over a 2-year period with no swelling, bulging or sagging in the silicone vessels. The major advantage of this method is that it allows for the fabrication of various levels of plaques and flexible to being modelled with different shapes and sizes. The phantom is robust, durable and provided good ultrasound measurements that matched that of the human carotid arteries.

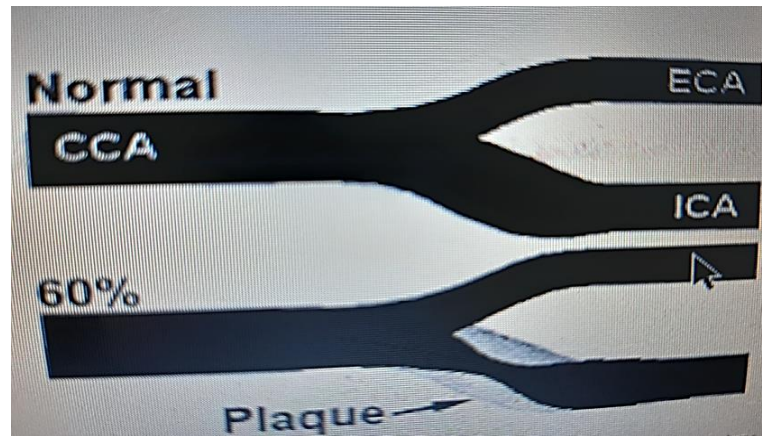


Figure 2.4: Carotid bifurcation models with normal geometry (top) and with a 60% stenosis (bottom) by NASCET criteria (Poeping *et al.*, 2004)

A walled phantom was designed to be applied in ultrasound assessment of wall motion of the artery (Dineley *et al.*, 2006). This phantom was made up of a straight tube representing the CCA and built with a polyvinyl alcohol cryogel (PVA-C) as the VMM enclosed by a TMM made from gelatine. The VMM and TMM were contained in a Perspex tank of length 320 mm, breadth 100mm and width 100 mm

connected at the inflow and outflow with a polyvinyl chloride (PVC) tube, 9.5 mm internal diameter. The BMF was pumped through the phantom with the aid of a magnetic gear pump. The TMM was a combination of 82.3% water, 13.1% gelatine, 3.4% glycerol and 0.87% CA24 preservative (Madsen *et al.*, 1986). A Philips HDI 5000 ultrasound scanner was used to obtain tissue Doppler imaging measurements. Results showed that the elastic modulus, acoustic velocity and attenuation coefficient varied from 57 kPa, 1543 ms<sup>-1</sup> and 0.18 dBcm<sup>-1</sup> MHz<sup>-1</sup> for one freeze-thaw cycle to 330 kPa, 1583 ms<sup>-1</sup> and 0.42 dBcm<sup>-1</sup> MHz<sup>-1</sup> for 10 freeze-thaw cycles respectively. All distension curves exhibited a rapid rise to a peak followed by a decrease in distension as the vessel wall contracted.

The results mean that the elastic modulus, speed of sound and attenuation of the vessel is a function of the number of freeze-thaw cycles. A good vessel made of PVA-C can be obtained at a freeze-thaw cycle numbers from 1 to 10 since the characteristics of the vessel are within acceptable standards (Cheng *et al.*, 1993; Loree *et al.*, 1994; Chu and Rutt, 1997; Debbich *et al.*, 2020). However, the effect of visco-elasticity on wall motion of the PVA-C phantom was not measured because the research was to produce physiologic distension waveforms only.

Another research was conducted by Wong *et al.*, 2008 on five (5) plastic materials to find out which of them is more suitable to be considered as a VMM. These materials are Teflon, Urethane-90A, Urethane-75D, Polyethylene of high density and polyethylene with high molecular weight. The acoustic properties of the 5 materials were determined by a pulse–transmission technique (Poepping *et al.*, 2004) at a frequency of 5 MHz. The vessel geometry chosen was a normal CCA with internal diameter of 8.0 mm and 50% stenosis at the bulb area as prescribed by the

NASCET criteria (Fox, 1993; Smith *et al.*, 1996; Smith *et al.*, 1999) . The experimental results revealed that Teflon was more suitable to be used as plastic material for flow phantoms because it had the best values for the speed of sound ( $1376 \pm 40 \text{ ms}^{-1}$ ) and attenuation ( $1.30 \pm 0.03 \text{ dBcm}^{-1}\text{Hz}^{-1}$  at 5 MHz) compared to the other four (4) plastics. Speed of sound is the primary acoustic property while attenuation is a secondary consideration in phantom fabrication (Holland *et al.*, 1984).

This explains the reason for selecting Teflon over other plastic materials even though its attenuation is higher compared to other materials. Plastic materials with very high speed of sound compared to international standard value ( $1540 \text{ ms}^{-1}$ ) results to phantoms with high refraction problems during ultrasound examinations. The phantom fabricated with Teflon in this experiment shows that Teflon provides the best combination of rigidity, reproducibility and DU compatibility, making it a suitable choice for the fabrication of rigid flow phantoms using a direct-machining method. The Teflon phantom also has the added advantage of an accurate and rapid fabrication process.

In yet another study, three phantoms were made from PVA-C with different stiffness (Qian *et al.*, 2014) fabricated to have properties the properties of a rubber from cryogel (Chu & Rutt, 1997). The solution was made from a combination of 10% PVA powder, 87% deionized water, and 3% of scatterers. The vessel had 6 mm inner diameter, 10 mm outer diameter, and 16 cm length. The phantoms were made by applying 3, 5 and 8 freeze-thaw cycles on the vessels moulds to produce 3 phantoms of different stiffness. The speed of sound and attenuation for the 3 phantoms were ( $1543.2 \text{ ms}^{-1}$ ,  $1.31 \text{ dBcm}^{-1}\text{MHz}^{-1}$ ), ( $1550.8 \text{ ms}^{-1}$ ,  $1.61 \text{ dBcm}^{-1}\text{MHz}^{-1}$ )

and ( $1552.1 \text{ ms}^{-1}$ ,  $1.70 \text{ dBcm}^{-1}\text{MHz}^{-1}$ ) for the 3, 5 and 8 freeze-thaw cycles respectively. These acoustic properties are closed to those of normal arteries (Greenleaf *et al.*, 1974; Hoskins, 2007). Measurements of the PSV and EDV were found to have magnitudes of 55.0 cm/s and 12.3 cm/s, 50.0 cm/s and 13.4 cm/s, and 44.9 cm/s and 14.8 cm/s in ascending order of stiffness. The results show that the acoustic properties and EDV increased with increase in the vessel stiffness, while the PSV decreases. Therefore, the design and fabrication process simulates blood flow in the artery properly. The use of test phantoms with different stiffness actually suggests that arterial stiffness has an impact on flow dynamics such as wall distension, flow pressure, time-dependent flow velocity and wall shear stress.

A decrease in wall shear rate was observed for a stiffer vessel, which may result to the pathological development of the endothelial cells in real vessels. The time to achieve peak systolic pressure in the pressure waveform coincided with the time to achieve maximum inner diameter in the wall distension waveform. This indicates that the wall motion and flow pressure occurred at the same time and frequency. For the pulsatile flow, the vessels underwent cyclic dilation and contraction during one cardiac cycle; the time-dependent curves of inner diameter increased from a minimum at end diastole to a maximum at peak systole, and then declined to the minimum. The recorded vessel wall distension waveform of the vessel is similar to that of an asymptomatic CCA (Dineley *et al.*, 2006). However, the use of micro-bubbles in aqueous solution as working fluid had lesser values of physical properties such as density and viscosity compared to real tissues thereby, influencing the distribution of the velocity flow and the wall shear stress.

A more robust method for fabricating anthropometric atherosclerotic phantoms was done using better ingredients for producing TMM and BMF (Galluzzo *et al.*, 2015). Computer aided manufacturing (CAM) software was used to realize a 3-D carotid artery phantom from which a mould was modelled consisting of an outer vessel mould (ABS plastic) and an inner core (soluble filament) to produce lumen of the artery. This method was used to produce two other phantoms with hyper echoic and hypo echoic plaques. The composition of the VMM, TMM and BMF are summarized in tables 2.3, 2.4 and 2.5 (Galluzzo *et al.*, 2015). The TMM ingredients were cooked until at  $96 \pm 3^\circ\text{C}$ , then allowed to cool down to  $42^\circ\text{C}$  before it was poured in a box containing the vessel phantom and left to solidify at about  $20^\circ\text{C}$  (Ramnarine *et al.*, 2001). The phantoms constructed properly simulate the lumen diameter of the real CCA, IMT and other hemodynamic indices comparable to normal arteries. This method of fabrication of anthropometric walled phantoms is very flexible in terms of applicability, less expensive, allows the study of cardiovascular diseases and provides extremely realistic ultrasound-based investigations.

Table 2.3: Percentage composition of substances used to prepare vessel mimicking material (VMM) and their uses in anthropometric atherosclerotic walled phantom (Galluzzo *et al.*, 2015)

| Name of Substance      | Percentage Composition (%) | Role of Substance                |
|------------------------|----------------------------|----------------------------------|
| De-ionized water       | 79.5                       | To serve as a solvent            |
| PVA powder             | 10.0                       | For gel formation                |
| Glycerol               | 10.0                       | To increase sound speed          |
| Aluminium Oxide powder | 2.0                        | To serve as scattering particles |
| Benzalkonium Chloride  | 0.05                       | To serve as anti-fungal agent    |

Table 2.4: Percentage composition of substances used to prepare tissue mimicking material (TMM) and their uses in anthropometric atherosclerotic walled phantom (Galluzzo *et al.*, 2015).

| <b>Name of Substance</b>      | <b>Percentage Composition (%)</b> | <b>Role of the Substance</b>                     |
|-------------------------------|-----------------------------------|--|
| De-ionized water              | 82.97                             | To serve as a solvent                            |
| Glycerol                      | 11.21                             | To measure the acoustic properties of the tissue |
| High gel-strength agar        | 3.0                               | For gel formation                                |
| Silicon Carbide               | 0.53                              | To serve as scatter particles                    |
| Aluminium Oxide (3 $\mu$ m)   | 0.94                              | To serve as scatter particles                    |
| Aluminium Oxide (0.3 $\mu$ m) | 0.88                              | To serve as scatter particles                    |
| Benzalkonium chloride         | 3.0                               | To serve as a preservative                       |

Table 2.5: Percentage composition of substances used to prepare blood mimicking fluid (BMF) and their uses in anthropometric atherosclerotic walled phantom (Galluzzo *et al.*, 2015).

| <b>Name of substance</b>                                       | <b>Percentage composition (%)</b> | <b>Role of substance</b>                         |
|--|-----------------------------------|--|
| Distilled water  | 83.86                             | Mimic the water component of blood               |
| 5 $\mu$ m Orgasol particles (2001 UDNAT1 Orgasol, ELF Atochem) | 1.82                              | Used as scatters                                 |
| Glycerol   | 10.06                             | To ensure appropriate density and speed of sound |
| Sigma D4786 dextran of average mw 150000D                      | 3,36                              | To increase the solution viscosity               |
| Synperonic A7 surfactant (Croda Health Care)                   | 0.9                               | To serve as surfactants                          |

In a similar research conducted by Adrian *et al.*, 2016, walled carotid artery phantoms for studying vessel wall motion and flow dynamics were fabricated with the aid of a computer and printing technology (3-D). The geometry consisted of CCA with 6-mm diameter, ICA with 4.2-mm diameter and ECA with 3.5-mm



diameter taking on a tuning fork model (Smith , 1999) with a thickness of 1.5 mm. The vessel branch parameters were defined such that they were in line with the mean carotid artery diameter of adults (Krejza *et al.*, 2006a). The vessel cores for carotid bifurcation models were made up of healthy and diseased geometries (25%, 50%, and 75% stenosis). The VMM mixture consisted of 86.7% distilled water, 10% PVA powder, 3% graphite with particle diameter less than 20  $\mu\text{m}$ , and 0.3% potassium sorbate, which served as an antimicrobial agent. The mixture was prepared in solution form at 90 °C under a double-boiler configuration and left to cool and settle for at least 12 h for easy degassing. The TMM was composed of 94.45% distilled water, 1.5% agar, 3.75% gelatine and 0.3% potassium sorbate preservatives. This mixture was made in solution form at 90 °C and after cooling to about 45°C, it was poured into an open volume of the phantom box and allowed to set at room temperature for 6 hours to form a congealed slab. The BMF was a solution of nylon scatterers solution (Ramnarine *et al.*, 1998). Test results conducted using the phantoms showed that the materials used in the fabrication process exhibit strong acoustic and physical compatibility for use in ultrasound imaging experiments more than the previously discussed phantoms. The speed of sound and attenuation for the TMM and VMM were  $1510 \pm 1.3 \text{ ms}^{-1}$ ,  $0.145 \pm 0.027 \text{ dBcm}^{-1}\text{MHz}^{-1}$  and  $1535 \pm 2.4 \text{ ms}^{-1}$ ,  $0.229 \pm 0.032 \text{ dBcm}^{-1}\text{MHz}^{-1}$  respectively. The phantom can suitably be used to carry out imaging of wall motion and flow dynamics using ultrasound methods.

Several other studies on in-vitro blood flow took their methods for fabricating walled human carotid artery phantoms from the above discussed methods (Onaizah *et al.*, 2017; Filippou and Tsoumpas, 2018; Chayer *et al.*, 2019; Elvira *et al.*, 2019) with the aid of CAD and 3-D printing technology. More applications of PVA-c and agar-based mixture for VMM fabrications together with the above methods of

preparing TMM and BMF are found in arterial phantoms with regional variations in wall stiffness and thickness (Chee *et al.*, 2018; Lai *et al.*, 2013)

### **2.2.3 (b) Wall-less Carotid Artery Phantoms**

Unlike walled phantoms, wall-less phantoms have their TMM in direct contact with the BMF (Ramnarine *et al.*, 2001) due to unsuitable VMM. They have the advantage of low attenuation coefficients and eliminating problems associated with different values of impedance between the tissues involved (Browne, 2014). However, wall-less vessels may be exposed to changes when the TMM is exposed to air or water. A wall-less test object was fabricated (Rickey *et al.*, 1995) to solve the problems of high rate of absorption, reflection and scattering common with walled phantoms using an agar-based TMM to replace the denser graphite by (Burlew *et al.*, 1980), hence ensuring proper suspension of the particles. The BMF was a mixture of distilled water, cutting fluid and nylon scatter particles. Results obtained from ultrasound measurements using this phantom were able to solve the above-mentioned problems.

About 20 years ago, advancements in the methodology for creating wall-less phantoms were carried out. One of such flow phantoms was designed with an agar-based TMM (Ramnarine *et al.*, 2001). It was made up of 82.97% water; 11.21% glycerol; 0.46% Benzalkonium Chloride; 0.53% 400 grain SiC powder; 0.94% of 3 mm Al<sub>2</sub>O<sub>3</sub> powder, 0.88% of 0.3 mm Al<sub>2</sub>O<sub>3</sub> powder and 3.00% Struers agar for rigidity. These components were heated in a double boiler at 96°C for about an hour and then allowed to cool down to 42°C with continuous stirring before finally pouring it into the container holding an 8-mm diameter straight rod. Reticulated foam of pore size 1–2 mm was fixed using Araldite adhesive around the inside and outside of the large inlet and outlet acrylic tubes.

This was done to prevent the BMF from leaking and to provide good rigid support to the small acrylic tubes for attachment to the flow circuit tubing. After the casted TMM had set and cooled, the rod was carefully removed allowing a hollow lumen (figure 2.5) for passage of the BMF (1.82% of  $5\ \mu\text{m}$  Orgasol particles; 83.86% of pure water; 10.06% of glycerol; 3.36% of Sigma D4876 dextran 185000D and 0.9% surfactant). All measurements of flow rates, velocities, attenuation and back scatter properties of the TMM and BMF using this phantom made the standard requirements by the International Electrochemical Commission 61685 (IEC, 2001). With continuous flow for some days, there was no leaking observed except for high backscatter signals possibly due to air bubbles and improper mixing during the preparation process. However, agar-based wall-less phantoms suffered from the limitation of rupture at high flow rates because of their shallow depths.

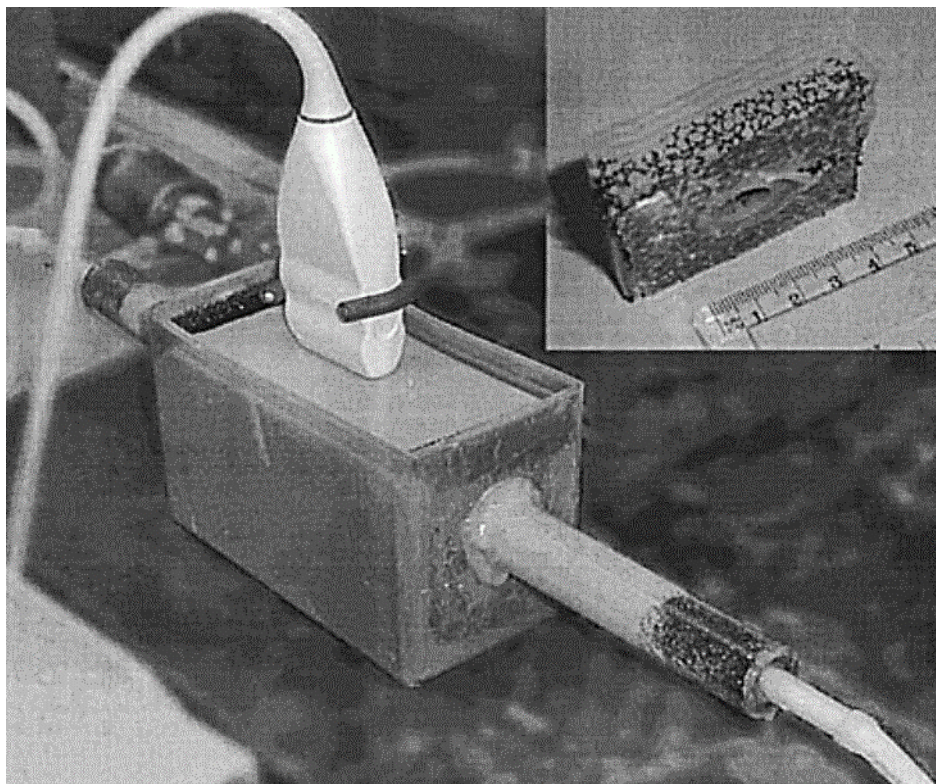


Figure 2.5: Photograph of flow phantom. Inset shows infiltration of TMM into reticulated foam (Ramnarine *et al.*, 2001).

A similar method for fabricating phantoms using the same ingredients for TMM and BMF by (Ramnarine *et al.*, 2001) was constructed consisting of three flow models of a 4.0 mm diameter, 4.6 mm diameter and 5.0 mm diameter CCA. These models were made up of agar for first size (wall-less model) and tubes for the other two with wall thicknesses of 0.8 mm and 1.0 mm respectively for assessing the performance of vessel wall tracking algorithms (Ramnarine *et al.*, 2004). Test using the TMM wall-less phantom gives low dilation during the wall tracking process probably due to acoustic mismatch problems. However, agar-based wall-less phantoms suffered from the limitation of rupture at high flow rates because of their shallow depths.

A Study on the use of konjac and carrageenan as constituents for preparing TMM was carried out by weight (Kenwright *et al.*, 2014). They found these powders suitable for gel formation with applications in both walled and wall-less phantoms at high frequencies of 5 – 60 MHz. This new recipe was used to construct phantoms with femoral artery (1mm diameter) and common carotid artery (2 mm diameter) of rats (Kenwright *et al.*, 2015). Other components of the TMM are summarized in table 2.6.

Table 2.6: Constituents of Konjac-Carrageenan based tissue mimicking material (TMM) for wall-les phantom (Kenwright *et al.*, 2014)

| Name of substance                              | Percentage Composition (%) | Function                                       |
|--|----------------------------|--|
| De-ionized water                               | 84.0                       | Serves as a solvent                            |
| Silicon Carbide                                | 0.53                       | Serves as scatters                             |
| Al <sub>2</sub> O <sub>3</sub> powder (3 μm)   | 0.96                       | Serves as scatters                             |
| Al <sub>2</sub> O <sub>3</sub> powder (0.3 μm) | 0.89                       | Serves as Scatters                             |
| Konjac powder                                  | 1.5                        | For gel formation                              |
| Carrageenan powder                             | 1.5                        | For gel formation                              |
| Potassium Chloride                             | 0.7                        | To fertilize the TMM                           |
| Glycerol                                       | 10.0                       | To mimic the acoustic properties of the tissue |

The prepared TMM with acceptable velocity of sound and attenuation was poured into the container of dimensions 10cm×10cm×23cm and allowed to set very well. A BMF (Ramnarine *et al.*, 1998) was pumped through the phantom using a gear pump. Acoustic properties were characterized using two methods; a broadband reflection substitution technique using a preclinical ultrasound scanner (Vevo 770, FUJIFILM VisualSonics, Toronto, ON, Canada), and a dedicated high-frequency ultrasound facility developed at the National Physical Laboratory (NPL, Teddington, UK), which employed a broadband through transmission substitution technique. The mean speed of sound across the measured frequencies and attenuation is found in table 2.7.

Table 2.7: Acoustic properties of TMM for broadband substitution and high frequency ultrasound methods

| Acoustic Properties                | Broadband reflection substitution method | High frequency ultrasound method |
|------------------------------------|--|----------------------------------|
| Attenuation (dBcm <sup>-1</sup> )  | 2.08±0.50                                | 1.58±0.30                        |
| Speed of Sound (ms <sup>-1</sup> ) | 1551.70 ± 12.70                          | 1547.70 ± 3.30                   |